Electronic Supplementary Material (ESI) for RSC Advances.

Electronic Supplementary Information

Efficient artificial light-harvesting system fabricated in aqueous media based on supramolecular polymers with AIE property

Tangxin Xiao,* Yong Shen, Cheng Bao, Kai Diao, Dongxing Ren, Hongwei Qian
and Liangliang Zhang

School of Petrochemical Engineering, Changzhou University, Changzhou, 213164, China.

E-mail: xiaotangxin@cczu.edu.cn

Table of contents

1. Materials, methods, and abbreviations

General

All chemicals, reagents and solvents were purchased from commercial suppliers and used, unless otherwise stated, without further purification. If needed, solvents were dried by literature known procedures. All yields were given as isolated yields.

NMR spectroscopy

The ^{1}H NMR spectra were recorded with a Bruker AVANCE III (300 MHz) and ^{13}C NMR spectra were recorded with a Bruker AVANCE III (500 MHz) spectrometer and calibrated against the residual proton signal or natural abundance carbon resonance of the used deuterated solvent from tetramethylsilane (TMS) as the internal standard. The chemical shifts δ are indicated in ppm and the coupling constants J in Hz. The multiplicities are given as s (singlet), d (doublet), t (triplet), and m (multiplet).

Mass spectrometry

High-resolution electrospray ionization mass spectra (HR-ESI-MS) were recorded on an Agilent Technologies 6540 UHD Accurate-Mass.

Transmission electron microscope (TEM)

TEM investigations were carried out on a JEM-2100 instrument.

Dynamic light scattering (DLS)

DLS measurements were carried out on a Brookhaven BI-9000AT system, equipped with a 200 mW polarized laser source ($\lambda = 514$ nm) at a scattering angle of 90°. All samples were prepared according to the corresponding procedures mentioned above.

UV-Vis spectroscopy

The UV-Vis absorption spectra were measured on a Perkin Elmer Lambda 35 UV-Vis Spectrometer.

Fluorescence spectroscopy

Fluorescence measurements were performed on an Agilent Cary Eclipse spectrofluorometer.

Fluorescence lifetimes

The fluorescence lifetimes were measured employing time correlated single photon counting on a FLS980 instrument with a pulsed xenon lamp. Analysis of fluorescence decay curves were subjected to fit a mono-exponential or bi-exponential decay. The instrument response function (IRF) measures the scattering of laser excitation from non-fluorescent control samples to determine the fastest possible response of the detectors.

Quantum yields

The quantum yields were carried out on a FLS980 instrument with the integrating sphere.

CIE coordinates

The CIE (Commission Internationale de l'Eclairage) 1931 coordinates were calculated with the method of color matching functions.

Viscometry

Viscosity measurements were carried out with Ubbelohde micro viscometers (Shanghai Liangjing Glass Instrument Factory, 0.40 mm inner diameter) at 298 K in chloroform.

Abbreviations

UPy = 2-ureido-4[1H]-pyrimidinone; NPs = nanoparticles; DCM = dichloromethane

$CHCl_3$ = trichloromethane; M = mol/L; br = broad; Ar = aromatic group

2. Specific viscosity of M

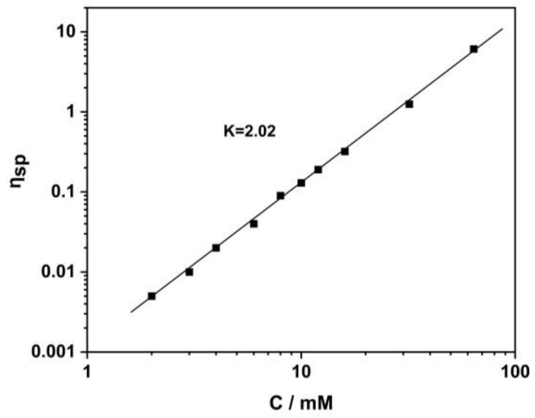

Fig. S1. Specific viscosity of **M** in $CHCl_3$ solutions versus the concentration (298 K). Values on the curves indicate the slope.

3. Fluorescence lifetime measurements

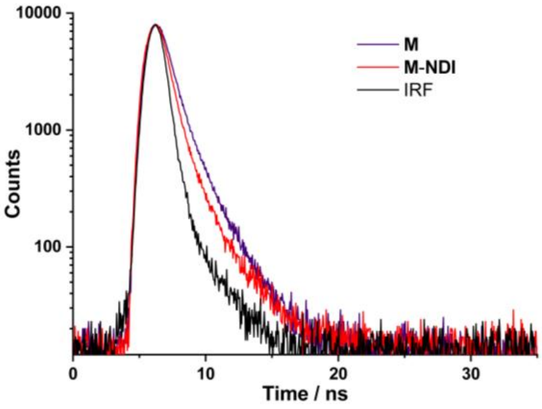

Fig. S2. Fluorescence decay profiles of NPs of **M** (blue line) and **M-NDI** (red line). λ_{ex} = 365 nm, [**M**] = 5×10^{-5} M, [**NDI**] = 5×10^{-7} M, respectively.

Table S1. Fluorescence lifetimes of **M-NDI** NPs (**M/NDI** = 100/1) upon excitation at 365 nm in aqueous solution, [**M**] = 5×10^{-5} M, [**NDI**] = 5×10^{-7} M, respectively.

Sample	**τ_1/ns**	**RW1**[%]	**τ_2/ns**	**RW2**[%]	**τ/ns**	χ^2
M	1.61	48.3	6.61	51.7	4.20	1.160
M-NDI (**M**: **NDI** = 100: 1)	0.60	31.8	4.87	63.2	3.30	1.095

4. Quantum yield measurements

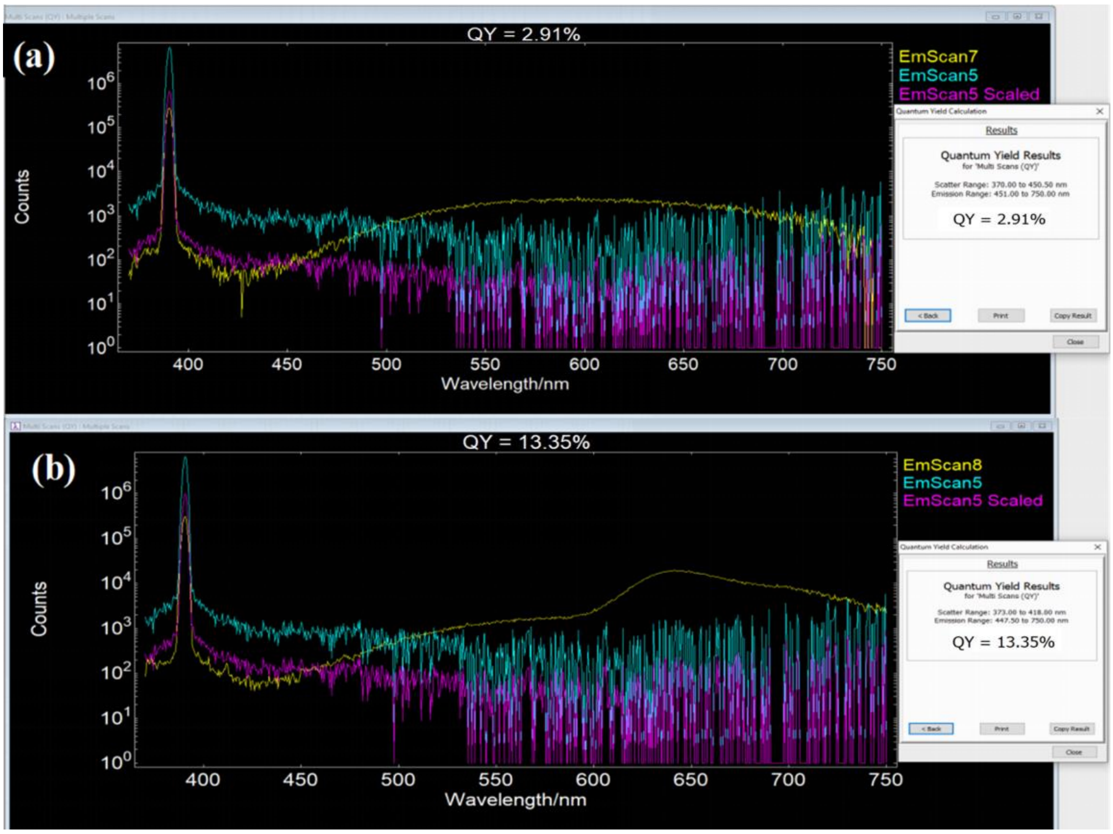

Results

Quantum Yield Results
for 'Multi Scans (QY)'

Scatter Range: 370.00 to 450.50 nm
Emission Range: 451.00 to 750.00 nm

QY = 2.91%

Results

Quantum Yield Results
for 'Multi Scans (QY)'

Scatter Range: 373.00 to 418.00 nm
Emission Range: 447.50 to 750.00 nm

QY = 13.35%

Fig. S3. Absolute fluorescence quantum yields ($\Phi_{f(abs)}$) of (a) NPs of **M**, (b) NPs of **M-NDI** (**M/NDI** = 100/1), upon excitation at 390 nm. [**M**] = 5×10^{-5} M, [**NDI**] = 5×10^{-7} M.

Table S2. Fluorescence quantum yields of NPs of **M** and **M-NDI**. [**M**] = 5×10^{-5} M, [**NDI**] = 5×10^{-7} M, respectively.

Sample	**Fluorescence quantum yields ($\Phi_{f(abs)}$)**
M	2.91%
M-NDI (**M: NDI =** 100: 1)	13.35%

5. Energy-transfer efficiency calculation

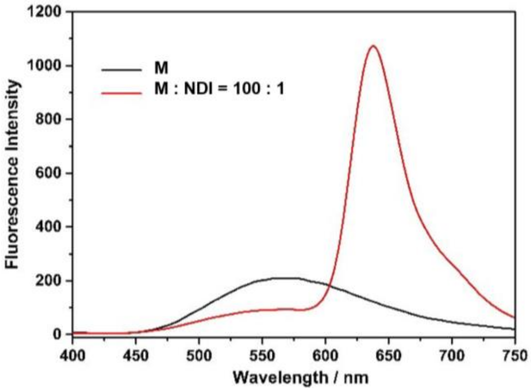

Fig. S4. Fluorescence spectra of **M** and **M-NDI** assembly upon excitation at 390 nm. NPs of **M** (black line), NPs of **M-NDI** (red line), respectively. [**M**]= 5×10^{-5} M, [**NDI**] = 5×10^{-7} M.

Energy-transfer efficiency (Φ_{ET}) was calculated from fluorescence spectra through the equation S1[S1]:

$$\Phi_{ET} = 1 - I_{DA} / I_D \text{ (eq. S1)}$$

Where I_{DA} and I_D are the fluorescence intensities of NPs of **M-NDI** (donor and acceptor) and NPs of **M** (donor) at 565 nm when excited at 390 nm, respectively.

The energy-transfer efficiency (Φ_{ET}) was calculated as 58.2% in water, measured under the condition of [**M**] = 5×10^{-5} M, [**NDI**] = 5×10^{-7} M, λ_{ex} = 390 nm.

Table S3. Energy-transfer efficiency with different D/A ratio.

Sample	**Concentration, respectively**	**Energy-transfer efficiency (Φ_{ET})**
M-NDI (**M**: **NDI** = 100: 1)	**[M]** = 5×10^{-5} M [**NDI**] = 5×10^{-7} M	58.2%
M-NDI (**M**: **NDI** = 150: 1)	**[M]** = 5×10^{-5} M [**NDI**] = 3.33×10^{-7} M	48.9%
M-NDI (**M**: **NDI** = 200: 1)	**[M]** = 5×10^{-5} M [**NDI**] = 2.5×10^{-7} M	38.3%
M-NDI (**M**: **NDI** = 300: 1)	**[M]** = 5×10^{-5} M [**NDI**] = 1.67×10^{-7} M	29.5%
M-NDI (**M**: **NDI** = 400: 1)	**[M]** = 5×10^{-5} M [**NDI**] = 1.25×10^{-7} M	23.9%
M-NDI (**M**: **NDI** = 500: 1)	**[M]** = 5×10^{-5} M [**NDI**] = 1×10^{-7} M	19.2%
M-NDI (**M**: **NDI** = 750: 1)	[**M**] = 5×10^{-5} M [**NDI**] = 6.67×10^{-8} M	11.5%
M-NDI (**M**: **NDI** = 1500: 1)	[**M**] = 5×10^{-5} M [**NDI**] = 3.33×10^{-8} M	10.7%
M-NDI (**M**: **NDI** = 3000: 1)	[**M**] = 5×10^{-5} M [**NDI**] = 3.67×10^{-8} M	7.4%

6. Antenna effect (AE) calculation

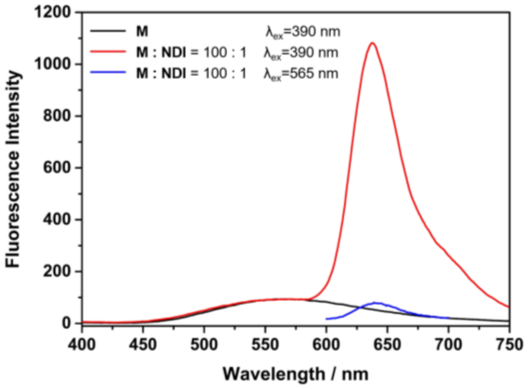

Fig. S5. Fluorescence spectrum of **M** NPs and **M-NDI** NPs normalized at 565 nm, **M** NPs (black line), **M-NDI** NPs (red line), respectively, λ_{ex} = 390 nm. The blue line represents the fluorescence spectrum of **M-NDI** NPs, λ_{ex} = 565 nm. [**M**]= 5×10^{-5} M, [**NDI**] = 5×10^{-7} M.

The antenna effect (AE) was calculated based on the emission spectra using equation S2[S1]:

$$AE = I'_{DA,390} / I_{DA,565} = (I_{DA,390} - I_{D,390}) / I_{DA,565} \text{ (eq. S2)}$$

Where $I_{DA,390}$ and $I_{DA,565}$ are the fluorescence intensities at 640 nm with the excitation of the light-harvesting NPs at 390 nm and at 565 nm, respectively. $I_{D,390}$ refers to the fluorescence intensity at 640 nm after the emission spectra of **M** NPs and **M-NDI** NPs are normalized at 565 nm under excitation at 390 nm.

The antenna effect value was calculated as 16.0 in water, measured under the condition of [**M**] = 5×10^{-5} M, and [**NDI**] = 1×10^{-7} M, respectively.

Table S4. Antenna effect with different donor/acceptor ratios.

Sample	Concentration, respectively	Antenna Effect (AE)
M-NDI (**M**: **NDI** = 100: 1)	[**M**] = 5×10^{-5} M [**NDI**] = 5×10^{-7} M	11.9
M-NDI (**M**: **NDI** = 150: 1)	[**M**] = 5×10^{-5} M [**NDI**] = 3.33×10^{-7} M	12.6
M-NDI (**M**: **NDI** = 200: 1)	[**M**] = 5×10^{-5} M [**NDI**] = 2.5×10^{-7} M	14.3
M-NDI (**M**: **NDI** = 300: 1)	[**M**] = 5×10^{-5} M [**NDI**] = 1.67×10^{-7} M	15.1
M-NDI (**M**: **NDI** = 400: 1)	[**M**] = 5×10^{-5} M [**NDI**] = 1.25×10^{-7} M	15.5
M-DBT (**M**: **DBT** = 500: 1)	[**M**] = 5×10^{-5} M [**NDI**] = 1×10^{-7} M	16.0
M-NDI (**M**: **NDI** = 750: 1)	[**M**] = 5×10^{-5} M [**NDI**] = 6.68×10^{-8} M	15.9
M-NDI (**M**: **NDI** = 1500: 1)	[**M**] = 5×10^{-5} M [**NDI**] = 3.33×10^{-8} M	15.3
M-NDI (**M**: **NDI** = 3000: 1)	[**M**] = 5×10^{-5} M [**NDI**] = 1.67×10^{-8} M	14.7

7. Control experiment of compound A for light-harvesting

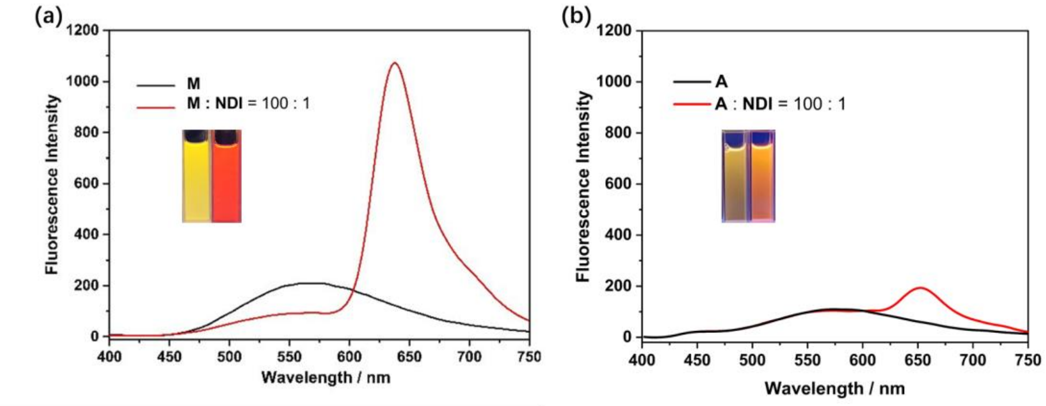

Fig. S6. (a) Fluorescence spectra of **M**, **M-NDI** upon excitation at 390 nm. (b) Fluorescence spectra of compound **A**, **A-NDI**. All these compounds are existed as NPs in water. [**M**] = 5×10^{-5} M, [**A**] = 5×10^{-5} M, [**NDI**] = 5×10^{-7} M, respectively.

8. Synthesis of compound M

A (2.58 g, 5.5 mmol) and **B** (3.60 g, 11.9 mmol) were dissolved in dry $CHCl_3$ (60 mL) and this solution was stirred for 12 h under nitrogen at room temperature. To the reaction mixture $CHCl_3$ (20 mL) was added and the organic layer was washed with 1 M HCl (80 mL × 1), saturated $NaHCO_3$ (80 mL × 3), brine (80 mL × 3), dried with anhydrous $MgSO_4$ and concentrated under reduced pressure. Added about 50 mL of methanol and heated to reflux 3 h, cool to room temperature, suction filter to obtain white powder (4.27 g, 4.51mmol). Yield: 82 %. ^{1}H NMR (300 MHz, $CDCl_3$): δ (ppm) = 13.22 (s, 2H, N*H*), 12.00 (s, 2H, N*H*), 10.37 (s, 2H, N*H*), 7.70 (d, *J* = 7.6 Hz, 2H, Ar-*H*), 7.25-7.19 (m, 6H, Ar-*H*), 6.99-6.90 (m, 6H, Ar-*H*), 6.81 (d, *J* = 7.8 Hz, 2H, Ar-*H*), 5.81 (s, 2H, alkene-*H*), 4.13 (t, *J* = 6.3 Hz, 4H, OCH_2), 3.56-3.48 (m, 4H, NCH_2), 2.33-2.25 (m, 2H, CH=CR-C*H*-R_2), 2.20-2.15 (m, 4H, alkyl-*H*), 1.71-1.50 (m, 8H, alkyl-*H*), 1.29-1.19 (m, 8H, alkyl-*H*), 0.90-0.82 (m, 12H, CH_2CH_3). ^{13}C NMR (125 MHz, $CDCl_3$): δ (ppm) = 173.2, 159.4, 156.9， 155.6, 154.9, 145.8, 140.1, 139.2, 135.5, 133.1, 131.9, 127.1, 126.2, 124.6, 119.2, 114.6, 106.3, 65.7, 45.4, 37.2, 32.9, 29.3, 29.2, 26.6, 22.5, 13.9, 11.7. HR-ESI-MS: m/z calcd for $[C_{56}H_{67}N_8O_6]^+$ = 947.5178, found = 947.5173.

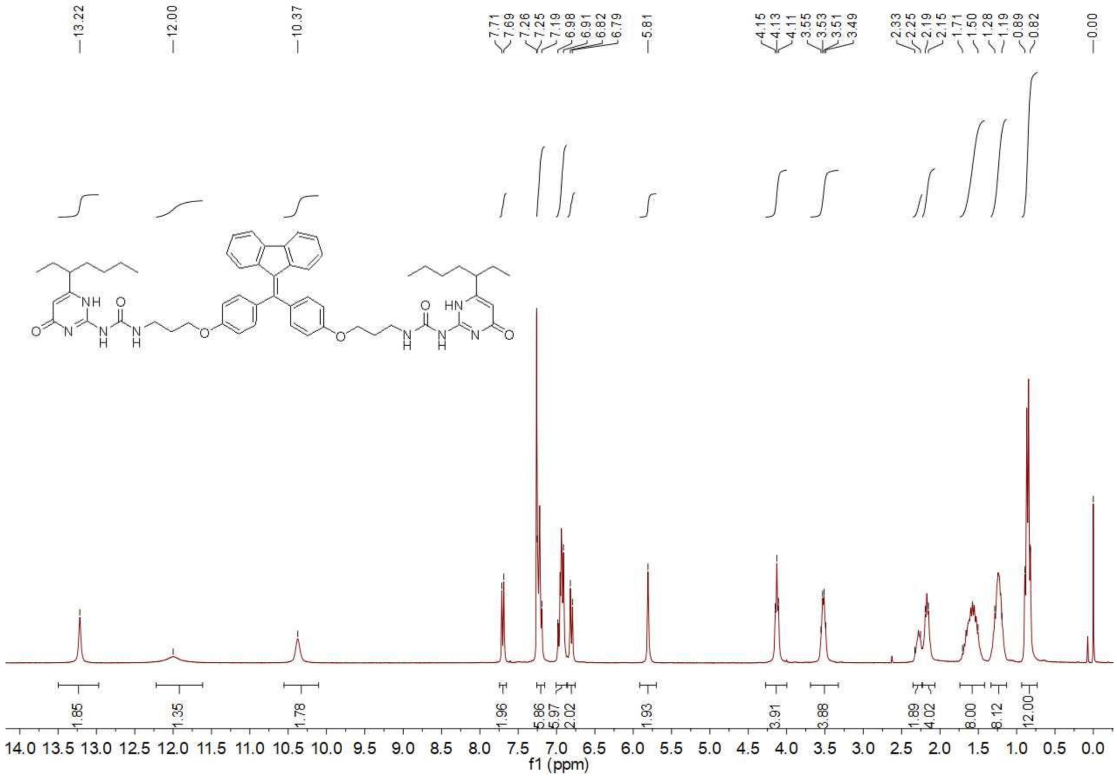

Fig. S7. ^{1}H NMR spectrum (300 MHz, CDCl$_3$, 298 K) of compound **M**.

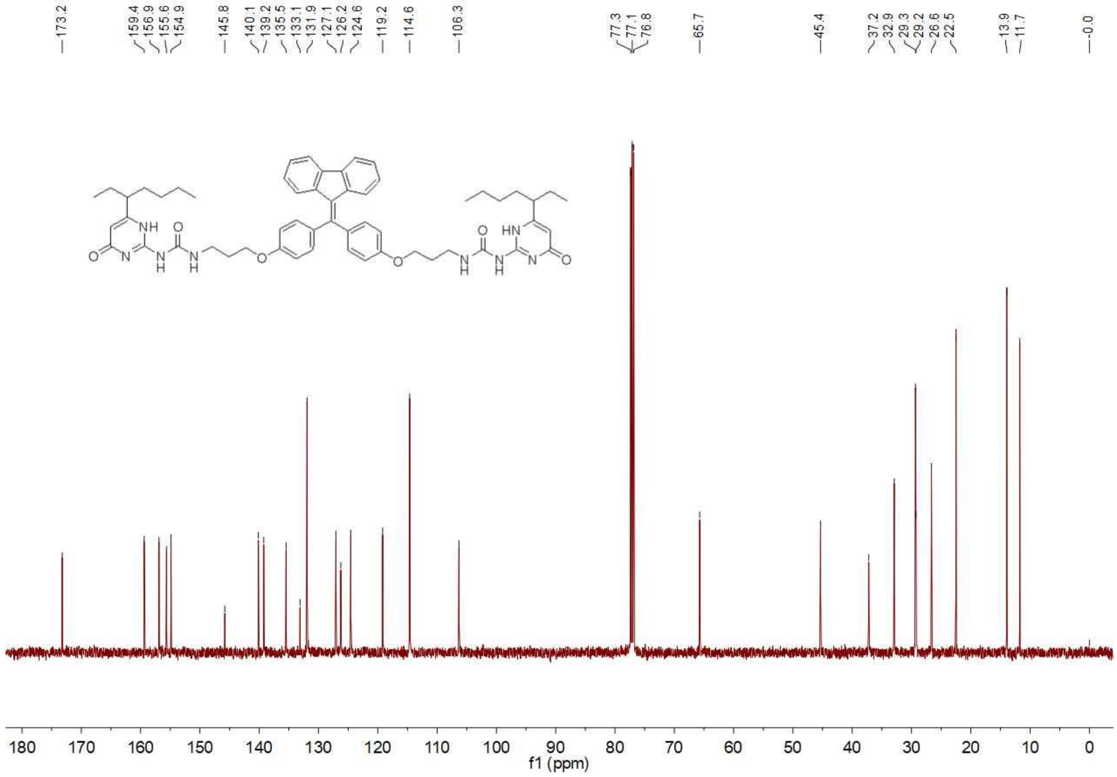

Fig. S8. ^{13}C NMR spectrum (125 MHz, CDCl$_3$, 298 K) of compound **M**.

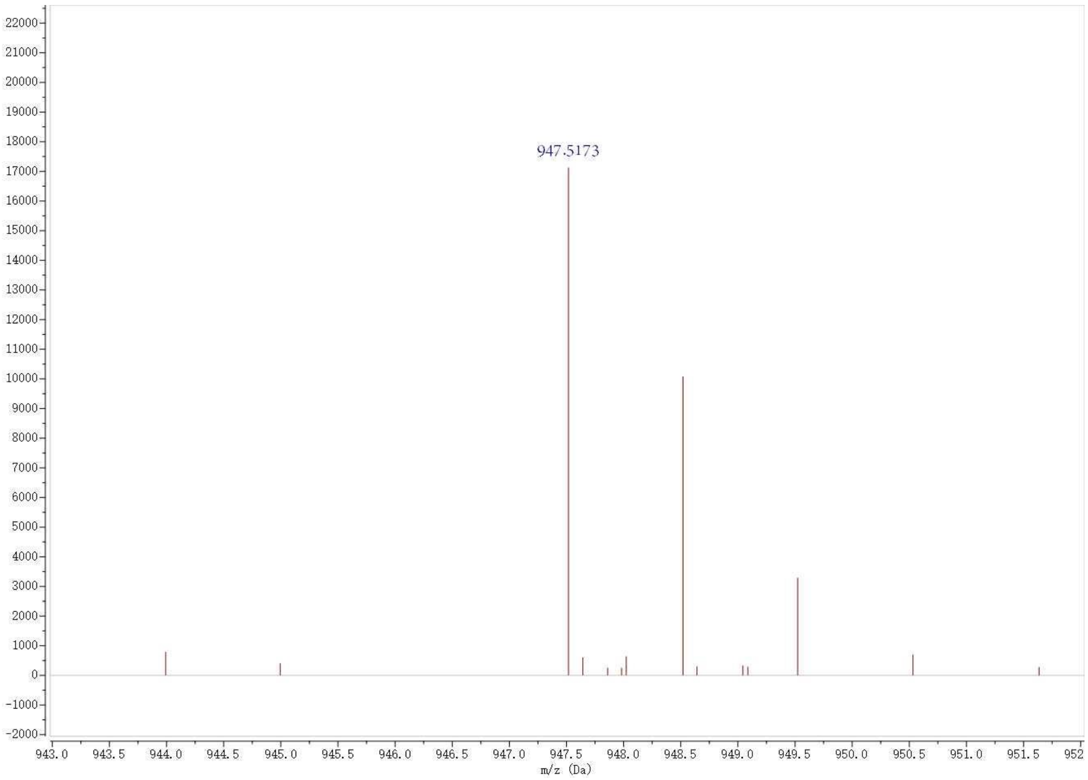

Fig. S9. HR-MS (ESI, positive mode, MeOH) of **M.**

9. References

[S1] Hao, M.; Sun, G.; Zuo, M.; Xu, Z.; Chen, Y.; Hu, X.-Y.; Wang, L. *Angew. Chem. Int. Ed.* 2020, **59**, 10095-10100.